# 7
# Plastic behaviour of nuclei and other finite systems

In some circumstances the nucleus acts as a liquid and in others like an elastic solid. In general it responds elastically to sudden forces, and it flows plastically over longer periods of time (Bertsch (1980, 1988)). Examples of this behaviour are giant resonances and low-lying collective surface vibrations respectively. In the first case, as we shall see in Section 8.3, pairing plays no role, at least in the case of nuclei lying along the valley of stability. The nuclear single-particle states change their shape but the occupation numbers do not change. The energy of a giant resonance in a nucleus is of the order of the energy difference between major shells ($\hbar\omega \approx 41/A^{1/3}$ MeV, $\approx 7$ MeV, for medium heavy nuclei), a quantity which is much larger than the pairing gap $\Delta \approx 1$–$1.5$ MeV. Giant resonances are fast modes, the collective motion is dominated by mean-field effects and the rigidity is provided by the mean field (Bortignon, Bracco and Broglia (1998)). On the other hand, low-energy surface modes are associated with particle–hole excitations which are of the order of the pairing gap. Pairing plays a dominant role and the collective states are coherent linear combinations of two-quasiparticle excitations. The situation is, however, different in the case of exotic nuclei, where the last nucleons are very weakly bound. Nucleon spill out makes these systems particularly polarizable leading to 'pigmy resonances', whose properties can be influenced by pairing (Frascaria *et al.* (2004), see also last paragraph of Chapter 6).

In any case, both giant resonances and surface vibrations can be treated in the harmonic approximation, and viewed as phonon excitations (see Chapter 8). Consequently, as in the case of the harmonic oscillator, associated with each degree of freedom of the vibrations there is a zero-point motion. In other words, the surface of a nucleus fluctuates in its ground state. The amplitude of these fluctuations is particularly important for low-lying quadrupole and octupole vibrations and somewhat less but still consistent for low-lying vibrations with multipolarity $\lambda = 4$ and $\lambda = 5$ (see Appendix C). In general these fluctuations

154

will be out of phase. However there is a finite although small probability that the fluctuations act coherently, allowing the system to probe large deformations. The presence of such deformations in the ground-state wavefunction is rather difficult to establish, as they act as virtual states which renormalize the properties of the ground state (see, however, Section 8.4).

## 7.1 Exotic decay

There are, however, exceptions to this situation, namely, in the case where the fluctuations lead to shapes corresponding to two daughter nuclei in a touching configuration, for which the $Q$-value associated with the division of the system is positive. In what follows we shall discuss an example of such a situation (see Fig. 7.1), namely the so-called exotic decay $^{223}Ra \rightarrow {}^{14}C + {}^{209}Pb$, a situation where pairing plays a central role in determining the inertia of the system.

A theory for the decay envisages two stages. In the first stage the nucleus evolves from a state with a moderate deformation to a cluster configuration like the one shown in Fig. 7.1 of touching parent–daughter nuclei. During this process pairs of nucleons change their states and the initial A-particle wavefunction $\phi_0$ evolves through local minima described by wavefunctions $\phi_i$, until it reaches the touching configuration described by the wavefunction $\phi_n$. In the deformation process the twofold degenerate single-particle levels (assuming axially symmetric deformation) will change their energy, those with wavefunctions along the poles decreasing their energy, while those along the equator will increase in energy as illustrated in the lower part of Fig. 7.2. At each crossing of an empty downsloping energy level and an occupied upsloping level two particles will
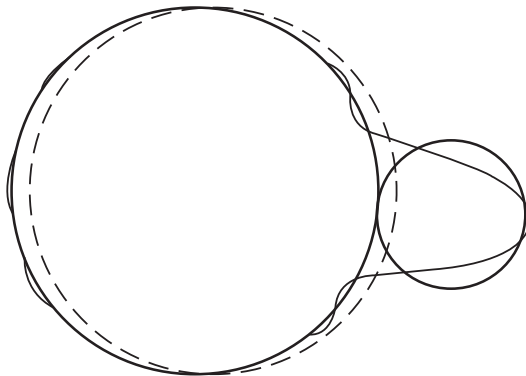


Figure 7.1. Shape transitions for the decay $^{223}Ra \rightarrow {}^{209}Pb + {}^{14}C$. The original nucleus is shown dashed; the touching daughter nuclei as heavy solid lines. The transformation described in the text carries the initial shape to the one shown by the light solid line (after Bertsch (1988), Barranco *et al*. (1990)).
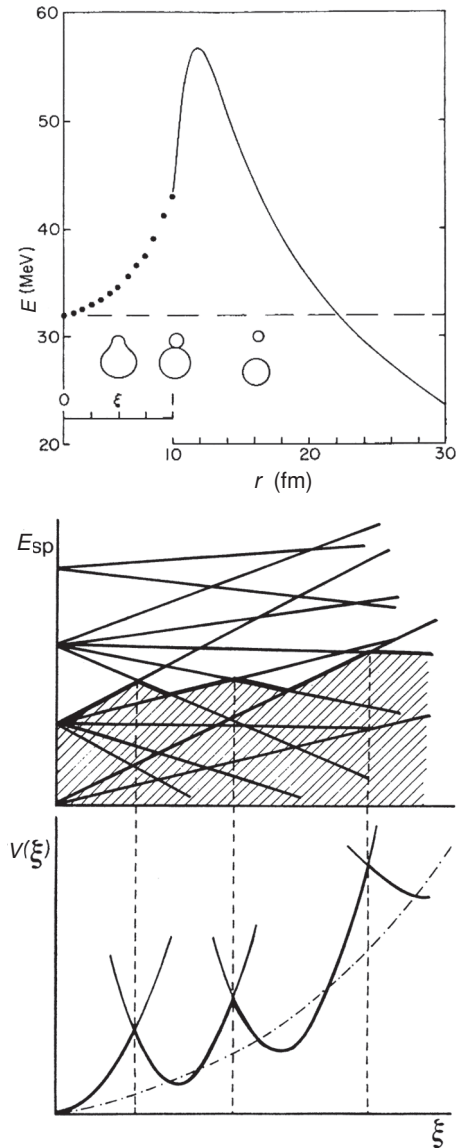
Figure 7.2. (Top) Potential energy curve for the decay $^{223}\text{Ra} \rightarrow {}^{209}\text{Pb} + {}^{14}\text{C}$. The outside potential is a combination of Coulomb and nuclear heavy ion potentials. The dots show the assumed Hartree–Fock states describing the shape change in the internal region. (Middle) Schematic representation of the occupancy of the single-particle levels. (Bottom) Local Hartree–Fock potential energies as a function of the deformation parameter $\xi$. Reprinted with permission from Barranco *et al.*, *Phys. Rev. Lett.* **60**:507–10 (1988a). Copyright 1988 by the American Physical Society.

change levels, under the action of the residual nuclear interaction, i.e. the part of the nuclear interaction not used in producing the mean field.

We assume that the wavefunction describing the evolution from the initial state $\phi_0$ to the final touching state $\phi_n$ is

$$\Phi = \sum_{i=1}^{n} a_i \phi_i, \tag{7.1}$$

where the $\phi_i$ are wavefunctions with pair correlations, like e.g. BCS wavefunctions, but with a number-projection so that there is a definite number of pairs in the upsloping levels and in the downsloping levels (see equation (4.45)). The suffix $n$ indicates the number of pairs transferred from the upsloping to the downsloping levels. The wavefunction $\phi_i$ describes the $i$th local minima in the potential energy diagram in Fig. 7.2 (bottom). The pairing interaction connects wavefunctions $\phi_i$ where the number of pairs changes from $i$ to $i \pm 1$. Consequently, the equation determining the ground-state wavefunction is the lowest-energy solution of the equation

$$\begin{bmatrix} \ddots & \vdots & \vdots & \vdots & \vdots \\ \cdots & E_{i-1} & v & \cdots & \cdots \\ \cdots & v & E_i & v & \cdots \\ \cdots & \cdots & v & E_{i+1} & \cdots \\ \vdots & \vdots & \vdots & \vdots & \ddots \end{bmatrix} \begin{bmatrix} \cdots \\ a_{i-1} \\ a_i \\ a_{i+1} \\ \cdots \end{bmatrix} = E \begin{bmatrix} \cdots \\ a_{i-1} \\ a_i \\ a_{i+1} \\ \cdots \end{bmatrix}. \tag{7.2}$$

The connection between equation (7.2) and a Schrödinger equation describing collective motion,

$$\left( -\frac{\hbar^2}{2D} \frac{d^2}{d\xi^2} + V(\xi) \right) \psi(\xi) = \mathcal{E}(\xi), \tag{7.3}$$

can be made discretizing equation (7.3) on a grid of step $\Delta\xi = 1/n$ in the interval $0 < \xi < 1$, using

$$\frac{d^2\psi}{d\xi^2} \approx \frac{\psi(\xi_{i-1}) + \psi(\xi_{i+1}) - 2\psi(\xi_i)}{\Delta\xi^2}.$$

Assuming that the deformation variable $\xi$ takes the value $\xi = 0$ for $\Phi = \phi_0$ ($^{223}$Ra in its configuration of minimum energy), and $\xi = 1$ for $\Phi = \phi_n$ ($^{209}$Pb and $^{14}$C at touching distance), one can write

$$M \begin{bmatrix} \cdots \\ \psi(\xi_{i-1}) \\ \psi(\xi_i) \\ \psi(\xi_{i+1}) \\ \cdots \end{bmatrix} = \mathcal{E} \begin{bmatrix} \cdots \\ \psi(\xi_{i-1}) \\ \psi(\xi_i) \\ \psi(\xi_{i+1}) \\ \cdots \end{bmatrix}, \tag{7.4}$$

where $M$ is the matrix

$$
\begin{bmatrix}
\vdots & \vdots & \vdots \\
V(\xi_{i-1}) + \frac{\hbar^2}{D\Delta\xi^2} & -\frac{\hbar^2}{2D\Delta\xi^2} & \cdots \\
-\frac{\hbar^2}{2D\Delta\xi^2} & V(\xi_i) + \frac{\hbar^2}{D\Delta\xi^2} & -\frac{\hbar^2}{2D\Delta\xi^2} \\
\cdots & -\frac{\hbar^2}{2D\Delta\xi^2} & V(\xi_{i+1}) + \frac{\hbar^2}{D\Delta\xi^2} \\
\vdots & \vdots & \vdots
\end{bmatrix}.
\tag{7.5}
$$

Comparing equations (7.2) and (7.5) one finds that the inertia of the system is

$$
D = -\frac{\hbar^2}{2v}n^2.
\tag{7.6}
$$

To use the above equation as a calculational tool we need to know the number of level crossings $n$ (see also Section 7.3) and the matrix element $v$. Before calculating the value of these parameters we note that the structure of this relation is quite plausible. The inertia is larger the larger the number of particles that have to be moved around in the motion. On the other hand, the larger the interaction, the smaller is the inertia, because it is easier to make a pair of particles jump at a crossing.

### 7.1.1 Inertia

It is fair to assume that the pairing residual interaction plays a central role in the process in which pairs of particles moving in time-reversal states change their state of motion. This is because pairing correlations lead to minimal friction. The pairing force Hamiltonian is

$$
H_{\mathrm{p}} = -GP^\dagger P = -G\left(P_{\mathrm{u}}^\dagger + P_{\mathrm{d}}^\dagger\right)(P_{\mathrm{u}} + P_{\mathrm{d}}).
$$

The transition matrix element between two successive states is

$$
v = \langle\phi_{i+1}|H_{\mathrm{p}}|\phi_i\rangle = -G\langle\phi_{i+1}|P_{\mathrm{d}}^\dagger P_{\mathrm{u}}|\phi_i\rangle,
$$

because a pair moves from an upsloping (u) level to a downsloping (d) level. It was shown in Chapter 3 that such transfer matrix elements can be estimated by mean values in BCS wavefunctions so that

$$
v \approx -G\langle\mathrm{BCS}|P_{\mathrm{d}}^\dagger|\mathrm{BCS}\rangle\langle\mathrm{BCS}|P_{\mathrm{u}}|\mathrm{BCS}\rangle
\tag{7.7}
$$

$$
\approx -\frac{G}{4}\langle\mathrm{BCS}|P|\mathrm{BCS}\rangle^2 = -\frac{1}{4}\frac{\Delta^2}{G},
$$

where we have assumed that

$$
\langle\mathrm{BCS}|P_{\mathrm{d}}^\dagger|\mathrm{BCS}\rangle = \tfrac{1}{2}\langle\mathrm{BCS}|P^\dagger|\mathrm{BCS}\rangle = \frac{\Delta}{2G}.
$$

We can state the result given in equation (7.7) in another way: a pairing force acting among all the downsloping and upsloping levels will give a matrix element which is the product of three factors: (i) the pairing force constant $G$, (ii) the probability (equal to $1/4$) that the initial states are occupied and the final is empty and (iii) the pairing enhancement factor $(\Delta/G)^2$. When both neutron and proton contributions are taken into account, equation (7.7) is modified to

$$v = -\left(\frac{\Delta_\nu^2 + \Delta_\pi^2}{4G}\right). \tag{7.8}$$

This same result has been derived in another way by Barranco *et al.* (1990). Employing the standard values $G = 25/A$ MeV, and $\Delta_\nu = \Delta_\pi = 12/\sqrt{A}$ MeV, one obtains

$$v = -2.9 \text{ MeV}. \tag{7.9}$$

To calculate $D$ we need now to know $n$, i.e. the number of pairs of particles which have to be moved around in $^{223}$Ra, to emit a $^{14}$C. Because the centre of mass of the total system has to remain at rest, fourteen particles have to be moved in one direction and fourteen in the opposite. Consequently, a fair estimate of $n$ is the reduced mass number of the process, i.e. $n \approx 13$. Finally,

$$D = -\frac{\hbar^2 n^2}{2v} = 29.1 \ \hbar^2 \text{ MeV}^{-1}. \tag{7.10}$$

We now proceed to estimate the potential energy $V$.

### 7.1.2 Potential energy

Assuming that the energies of the different local minima lie on a parabola (see Fig. 7.2 (bottom)), one can write

$$V(\xi) = \tfrac{1}{2} C \xi^2. \tag{7.11}$$

An expression for the potential at $\xi = 1$ can be read off from the sketch in the upper part of Fig. 7.2

$$V(\xi = 1) + Q = U_{aA}^c(R_0) + U_{aA}^N(R_0), \tag{7.12}$$

where $R_0$ is the distance at which the two densities barely touch, i.e. $R_0 = R_a + R_A + a$, $R_i$ being the radius of $^{14}$C ($i = a$) and of $^{209}$Pb ($i = A$). The diffusivity of the ion-ion potential $U_{aA}^N$ is denoted by $a$, while $U_{aA}^c$ is the Coulomb potential acting between the ions. Finally, the quantity $Q = 31.9$ MeV is the Q-value of the decay process.

The decay rate is very sensitive to the parameters of the potential barrier outside the touching radius. Here we follow Barranco *et al.* (1988a, 1990), and

use the Christensen–Winther potential (Broglia and Winther (1991))

$$U_{aA}^N = S_0 \bar{R}_{aA} \exp\left(-\frac{r-R}{a}\right), \tag{7.13}$$

which gives a good description of heavy ion elastic scattering and fusion reactions. The radius parameters $R$ and $\bar{R}_{aA}$ in (7.13) are defined by

$$\bar{R}_{aA} = \frac{R_a R_A}{R_a + R_A}, \quad R = R_a + R_A. \tag{7.14}$$

where $R_a$ and $R_A$ of the two nuclei are parametrized according to

$$R_i = (1.233 A_i^{1/3} - 0.98 A_i^{-1/3}) \text{ fm}, \tag{7.15}$$

and the values $S_0 = -50 \text{ MeV fm}^{-1}$, $a = 0.63 \text{ fm}$ are used. Substituting the numerical values into equation (7.13) one obtains

$$U_{aA}^N(r) = -94 \exp\left(-\frac{r-9.7}{0.63}\right) \text{ MeV}, \tag{7.16}$$

and

$$V(\xi = 1) = U_{aA}^c(10.5) + U_{aA}^N(10.5) - 31.6 \text{ MeV} = 9.2 \text{ MeV} \tag{7.17}$$

leading to

$$C = 18.4 \text{ MeV}. \tag{7.18}$$

### 7.1.3 Formation probability

The wavefunction describing the ground state of the harmonic oscillator is

$$\psi(\xi) = \left(\frac{\alpha}{\sqrt{\pi}}\right)^{1/2} e^{-\frac{1}{2}\alpha^2 \xi^2}, \tag{7.19}$$

where

$$\alpha^2 = \frac{D\omega}{\hbar} = \sqrt{\frac{DC}{\hbar^2}} = \sqrt{\frac{C}{2|v|}} n \approx 23.2. \tag{7.20}$$

Consequently, the formation probability is

$$P = |\psi(\xi = 1)|^2 = \frac{\alpha}{\sqrt{\pi}} e^{-\alpha^2} = 2.4 \times 10^{-10}. \tag{7.21}$$

That is, the ground state of $^{223}$Ra acquires shapes resembling the touching configuration of $^{209}$Pb and $^{14}$C with the probability (7.21).

### 7.1.4 Decay constant

Once the $^{14}$C is formed, the decay process can be described in terms of the standard Gamow theory, i.e. in terms of a knocking rate $f$ and a tunnelling factor $T$, the associated decay constant being

$$\lambda = PfT. \tag{7.22}$$

Before proceeding to the calculation of $f$ and $T$, we want to make a short remark on the standard theory of alpha decay, where one assumes $P = 1$. The reason why this approach to alpha decay is able to provide an overall account of the experimental findings is because in this case the preformation factor is of the order of 1 ($P \approx 10^{-1}$), and the tunnelling probability $T$ (or $\gamma$ in the standard language) is a very sensitive function of the input parameters. Any uncertainty in $P$ can be compensated by a small change in the radius and height of the Coulomb barrier.

### 7.1.5 Knocking rate

To estimate $f$ one makes the standard assumption of motion of a particle of inertia $D$ in the ground state of a harmonic well. Then

$$\omega = \sqrt{\frac{C}{D}} = 1.2 \times 10^{21} \text{s}^{-1} \tag{7.23}$$

and

$$f = \frac{\omega}{2\pi} \approx 2 \times 10^{20} \text{s}^{-1}. \tag{7.24}$$

### 7.1.6 Tunnelling probability

We have to calculate the probability for tunnelling the Coulomb barrier starting from the touching distance $R_0 \approx 10.3$ fm. A convenient analytic formula is obtained neglecting the nuclear potential (Tonozuka and Arima (1979)):

$$T = \frac{kR_0}{F_0^2(kR_0) + G_0^2(kR_0)}, \tag{7.25}$$

in terms of the regular and irregular Coulomb functions. In equation (7.25) $k$ is given by

$$k = \sqrt{\frac{2M_{aA}}{(E_B - Q)}\hbar^2}. \tag{7.26}$$

The height of the Coulomb barrier is given by (Broglia and Winther (1991))

$$E_{\mathrm{B}} = \frac{Z_a Z_A e^2}{r_{\mathrm{B}}}\left(1 - \frac{0.63}{r_{\mathrm{B}}}\right) \approx 58 \text{ MeV}, \tag{7.27}$$

where the associated radius is given by

$$r_{\mathrm{B}} = 1.07(A_a^{1/3} + A_A^{1/3}) + 2.72 \text{ fm} \approx 11.6 \text{ fm}. \tag{7.28}$$

One finally obtains from equation (7.25)

$$T \approx 10^{-26}. \tag{7.29}$$

### 7.1.7 Comparison to experiment

Making use of the relation (7.22) and of the quantities (7.21), (7.24) and (7.29), one obtains the theoretical value

$$\lambda_{\mathrm{th}} \approx 10^{-16} \text{ s}^{-1}, \tag{7.30}$$

to be compared with the experimental value (Rose and Jones (1984)) of

$$\lambda_{\mathrm{exp}} = 4.3 \times 10^{-16} \text{ s}^{-1}. \tag{7.31}$$

One has to keep in mind that no calculation can predict a decay constant with an accuracy better than 1–2 orders of magnitude.

The theory presented here is based on the idea that the parent nucleus evolves from an initial state with a moderate deformation to a cluster configuration by a series of level crossings. The calculated preformation factor is $P \approx 10^{-10}$. Other theories suppose that the cluster structure exists in the parent nucleus so that the preformation factor $P = 1$. Theories with widely different preformation factors are able to fit the data because of the extreme sensitivity of the penetration factor to the barrier parameters. For example Buck and Merchant (1989) use a potential with a barrier height of 63.9 MeV and radius 10.2 fm for the cluster decay of $^{223}$Ra instead of the Christensen and Winther values $E_{\mathrm{B}} = 58$ MeV and $r_{\mathrm{B}} = 11.6$ fm. An increase of the barrier height of 6 MeV decreases the penetration factor by a factor of $10^{10}$ and compensates for the increase in the penetration factor. They have also been able to fit many other exotic decays. Buck *et al.* (2000) have a method for predicting the cluster structure of a nucleus by relating it to the decay $Q$-value. One argument in favour of the approach in the present chapter is that the Christensen-Winther potentials fit heavy ion elastic scattering data. This aspect has not been studied for the potentials used by Buck and his collaborators. Another argument is that the superfluid tunnelling model discussed in the present chapter can also be applied to other processes.

Table 7.1. *The four decay modes of* $^{234}$U *(after Broglia et al. (1993)).*

| Decay | $\lambda_{exp}(s^{-1})$ | $\lambda_{th}(s^{-1})$ | $n$ |
|---|---|---|---|
| $^4$He | $9. \times 10^{-14}$ | $2. \times 10^{-14}$ | 4 |
| $^{24}$Ne | $6.3 \times 10^{-26}$ | $1. \times 10^{-28}$ | 19 |
| $^{28}$Mg | $2. \times 10^{-26}$ | $2. \times 10^{-28}$ | 23 |
| spont. fission | $(8.6 \pm 1.8) \times 10^{-24}$ | $5. \times 10^{-24}$ | 52 |

## 7.2 A variety of applications

The superfluid tunnelling model has been applied to a variety of problems involving the evolution of the nuclear system between two minima. In particular:

(1) To the calculation of alpha and exotic decay as well as fission, where the model provides an overall account of the data over twenty orders of magnitude (Barranco *et al.* (1990)); in particular a quantitative picture of the four decay modes of $^{234}$U (see Table 7.1) (Barranco *et al.* (1989)), as well as the correction of the chart of nuclides regarding the lifetime quoted for the spontaneous fission of $^{232}$U. The model predicts in fact an exotic decay branch $^{232}$U $\rightarrow$ $^{208}$Pb + $^{24}$Ne which is close to the experimental value (Bonetti *et al.* (1990)), and to the 1990 'fission' value. The prediction of the model ($\lambda_{SF} = 5 \times 10^{-24}$ s$^{-1}$) of the spontaneous fission decay rate was found to be in agreement with experiment (Bonetti *et al.* (2000)).

(2) To the decay of superdeformed bands (Herskind *et al.* (1988)). Although the superdeformed minimum lies, as a rule, above the normal deformed minimum for spins less than 50 $\hbar$, its population is not affected down to spin of about 24 $\hbar$, where the sudden transition out of the superdeformed band observed in experiment can be related to the onset of pairing caused by the disalignment of the lowest pair of high-$j$ particles (see Section 6.5).

(3) To the restoration of parity conservation in octupole deformed nuclei (Barranco *et al.* (1988b,c)). The potential energy surface of a superfluid nucleus with an even multipole deformation has, as a rule, a single absolute minimum as a function of the deformation. For odd multipole deformations, there will be two minima with mirror image wavefunctions. This is a basic requirement of quantum mechanics as the physical states must be eigenstates of the parity operator. In an octupole deformed nucleus, this is achieved by a tunnelling of the system between the minima. This tunnelling is connected with the interaction between odd- and even-parity rotational bands. In the particular case of $^{222}$Ra it is experimentally found that the excitation of the first negative parity state is at $\Delta E = 242$ keV above the positive $0^+$ ground state. The model predicts a value of $\Delta E$ lying between 150 and 500 keV, depending on the potential energy

surface used. In fact, in this case, because the number of steps is small, the result is rather sensitive to the details of the calculation.

(4) To the calculation of the lifetime of high $K$-isomer states in rotating nuclei (Bengtsson *et al.* (1989)), such as $^{182}$Os. There is overwhelming experimental evidence which testifies to the fact that cold, deformed nuclei display axially symmetric quadrupole deformations. Therefore the projection of the angular momentum on the body-fixed symmetry axis is a conserved quantity, and its value $K$ is a good quantum number (Bohr and Mottelson (1975)). In keeping with this fact, excited states with high $K$-values are often isomeric, decaying only by virtue of small admixtures of lower-$K$ components. A consequence of the $K$-selection rule is that the decay from the high $K$-states takes place preferentially stepwise, and degrees of $K$-forbiddenness vary from 5 to 100 for each step $\Delta K = 1$. The decay of an isometric state with $I^\pi = 25^+$ has been observed in $^{182}$Os, directly populating the state of the yrast band ($K = 0$), with a hindrance factor of $10^{-8}$. One single transition thus changes $K$ dramatically, and with an isomeric lifetime that is relatively short.

Interpreting the isomer as a rotation around the symmetry axis, i.e. where all the angular momentum is contributed by the particles (see Fig. 6.1 (right)), one has to deal with a tunnelling in the gamma degree of freedom (Bohr and Mottelson (1975)). Estimates making use of the superfluid tunnelling model lead to a hindrance factor of the order of $10^{-6}$–$10^{-9}$, where the uncertainty is connected with poor knowledge of the potential around the $K$-isomer minimum.

(5) To the calculation of the deformation and of the energy of coexistence states (four-particle–four-hole excitations) in $^{16}$O and $^{40}$Ca (Bertsch (1980)). The evolution of the system from one local minimum to the next implies a change in the deformation such that the energy associated with the lowest 2p–2h excitation becomes zero. That is, a deformation leading to a crossing between the lowest empty and the lowest occupied single-particle state. In the case where the deformation has quadrupole multipolarity, and is axially symmetric, the relation between the number of level crossings $n_2$ and the deformation $\beta_2$ in a nucleus of mass number $A$ is given by $\beta_2 = 2(12\pi/5)^{1/2}n_2/A$ (see equation (7.35)). Because each level is twofold degenerate, to produce a 4p–4h excitation one needs a deformation corresponding to $n_2 = 2$. This implies $\beta_2 = 0.7$ for $^{16}$O and $\beta_2 = 0.3$ for $^{40}$Ca, compared with the values of 0.84 and 0.27 deduced from the experimental evidence. A rough estimate of the energy can be obtained by calculating the change in surface tension associated with these deformations. Making use of the liquid drop model (see equation (7.32)), this change is $\Delta E = 1/2C_2\beta_2^2 \approx 2\beta_2^2 R_0^2 S$, where $R_0 = 1.2A^{1/3}$ fm is the nuclear radius, $S = 0.95$ MeV fm$^{-2}$ is the surface tension and the Coulomb correction to $C_2$ has been neglected. From this relation and the above deformation parameters one obtains 8 and 3 MeV respectively, compared with the experimental values of 6.1 and 3.4 MeV.

## 7.3 Low-lying surface vibrations

In most cases the lowest excited states of even–even nuclei have a quadrupole or octupole character (Bohr and Mottelson (1969, 1975)). Although these states carry a small fraction (5–10%) of the energy weighted sum rule (see Section 8.3.2), the associated transition probabilities are much larger than that of single-particle states. Furthermore, they are excited with large cross-section by projectiles which are absorbed at the nuclear surface. They are known as collective surface vibrations, and are intimately connected with the plastic behaviour of the atomic nucleus.

Consequently, we shall use, in the calculation of the frequencies of these modes, the same scheme used to discuss exotic decay in Section 7.1 (Broglia *et al.* (1994)). The two parameters entering the model are the restoring force $C_L$ and the inertia $D_L$ of the mode. Because we are dealing with the plastic behaviour of the system one can use the liquid drop model to calculate $C_L$. In fact, in a vibrational motion where the surface fluctuates with a frequency of the order of $10^{21}$ s$^{-1}$, the detailed motion of the nucleons associated with frequencies almost two orders of magnitude larger must be quite irrelevant. Consequently, the surface tension $S$ ($\approx 0.95$ MeV fm$^{-2}$) is sufficient to characterize the deformation energy of the system, and the restoring force parameter can be written as (Bohr and Mottelson (1969, 1975)),

$$C_L = S(L-1)(L+2)R_0^2 - \frac{3}{2\pi}\frac{L-1}{2L+1}\frac{e^2Z^2}{R_c} . \qquad (7.32)$$

The two radii in the expression are the nuclear and the Coulomb radii, $R_0 = 1.2A^{1/3}$ fm and $R_c = 1.25A^{1/3}$ fm, respectively, $A$ being the mass number. The quantity $Z$ indicates the proton number of the system. In what follows we shall use the approximate relation $Z \approx A/2.4$ (see Section 3.5). In this way one obtains

$$\frac{C_L}{A^{2/3}} = \begin{cases} 5.4(1-0.003A)\,\text{MeV} & (L=2), \\ 13.5(1-0.002A)\,\text{MeV} & (L=3), \\ 38(1-0.0005A)\,\text{MeV} & (L=5). \end{cases} \qquad (7.33)$$

For the inertia we use

$$\frac{D_L}{\hbar^2} = -\frac{1}{2v}\left(\frac{dn}{d\beta_L}\right)^2, \qquad (7.34)$$

where $v = -2.9$ MeV and $dn/d\beta_L$ is the density of level crossings per unit deformation. In Section 7.1, where the phenomenon of exotic decay has been discussed, we have used a simplified version $dn/d\beta_L$ which, in that case is determined by the reduced mass number of the exotic decay products. In the present case we do not have any direct experimental input to calculate $dn/d\beta_L$, and have to work it out theoretically.

The quantity $dn/d\beta_L$ can be estimated quite accurately by realizing that the Fermi distribution in momentum space is spherical for each local minimum (Bertsch (1980, 1988)). Between crossings, the Fermi surface gets distorted. In fact, it elongates in correspondence to a spatial reduction of the nuclear radius and it retracts when the nuclear radius becomes larger. Each time the volume outside the original Fermi sphere contains two nucleons, it is possible to fill the depopulated momentum zones below the Fermi energy and restore spherical symmetry. This means that the system has moved from a local minimum to the nearest one, and that a pair of nucleons have changed orbital. Making use of such a model one obtains for $L \lesssim 5$ the approximate expression (Bertsch (1988))

$$\frac{dn}{d\beta_L} \approx \frac{1}{4}\sqrt{\frac{2L+1}{3\pi}}A. \tag{7.35}$$

We are now in a position to calculate the inertia of the modes

$$\frac{D_L}{\hbar^2} \approx (2L+1)10^{-3}A^2 \, \text{MeV} . \tag{7.36}$$

The basic frequencies associated with the low-lying collective vibrations $L = 2, 3, 4$ and $5$ are thus

$$\hbar\omega_L = \sqrt{\frac{\hbar^2 C_L}{D_L}} \approx \sqrt{\frac{(L-1)(L+2)}{(2L+1)}}(1-0.001A)\frac{35}{A^{2/3}} \, \text{MeV} . \tag{7.37}$$

In Figs. 7.3 and 7.4 we show the function given in equation (7.37) for $L = 2$ and $L = 3$ in comparison with the experimental findings. Although large fluctuations
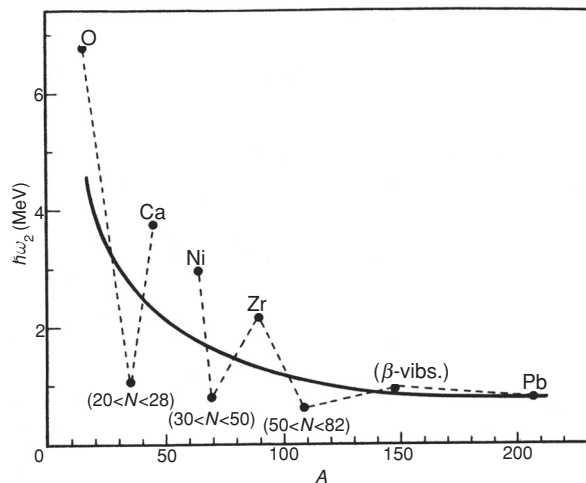


Figure 7.3. Average energy of the lowest $2^+$ state in nuclei as a function of the mass number. The data are taken from Bohr and Mottelson (1969), Table 2.17 p. 196. The dashed line is to guide the eye. The continuous curve was calculated making use of equation (7.37) setting $L = 2$.

Figure 7.4. The same as in Fig. 7.3, but for $L = 3$. The data are taken from Bohr and Mottelson (1975) Fig. 6.40 p. 560.

about the theoretical value are observed, because shell effects greatly affect pairing correlations in nuclei (see also Chapter 10, Figs. 10.6–10.8), the result given in equation (7.37) provides an overall account of the experimental findings.

The amplitude of the zero-point motion associated with these modes is given by

$$\frac{\beta_L}{\sqrt{2L+1}} = \sqrt{\frac{\hbar\omega_L}{2C_L}} = \frac{3.6A^{-2/3}}{[(L-1)(L+2)(2L+1)]^{1/4}}. \tag{7.38}$$

From the above equation and from equation (7.35) one can estimate that the number of crossings associated with the vibrational modes of energy given in equation (7.37) is

$$n \approx \left(\frac{(2L+1)^3}{(L-1)(L+2)}\right)^{\frac{1}{4}} 0.3A^{1/3} \approx 0.5A^{1/3}. \tag{7.39}$$

Making use of $A^{1/3} \approx 5$ for medium-heavy nuclei, one obtains $n \approx 3$, an estimate which provides a quantitative justification for the use of a large amplitude description for low-lying surface vibrations of atomic nuclei. A detailed account of the low-lying collective surface vibrations taking into account shell effects is provided by the quasiparticle random phase approximation (QRPA) (see equation (8.47)).

## 7.4  Fission in metal clusters

Metal clusters have been investigated systematically during the past years. They are aggregates of metallic atoms, displaying clear shell structure. In particular, microclusters of sodium atoms can be viewed as a system of delocalized electrons, moving in single-particle orbits. An approximation for the description of the clusters is provided by the jellium model where the positive charge of the ions is assumed to be uniformly distributed over the cluster volume. The motion of the electrons can be described by a single-particle potential, arising from the interplay between the attractive jellium background, the Hartree–Fock potential and the correlation energy calculated in the local density approximation (LDA). In particular the shell closures, which in the case of Na clusters start with the magic numbers 8, 20 and 40, are well reproduced (see de Heer and Knight (1988), Broglia *et al.* (2004)).

Based on this picture one can explore analogies between metal clusters and nuclei. One example is the fission of a metal cluster, called a Coulomb explosion. The reason for this name is that clusters with almost any number of electrons can be made to fission, by charging them positively (see Eckhardt (1984)). Local-spin-density molecular dynamics calculations (Saunders (1990), Barnett *et al.* (1991)) predict the asymmetric fission of small doubly charged sodium (Na) clusters to occur predominantly via $Na_n^{+2} \rightarrow Na_{n-3}^+ + Na_3^+$, for $4 \leq n \leq 12$. For $n$ less than or equal to 6, no fission barrier is present, while fission of larger clusters involves a barrier. The largest barrier for the range of clusters investigated is in the case of the process

$$Na_{10}^{+2} \rightarrow Na_7^+ + Na_3^+, \tag{7.40}$$

and is associated with the closed shell produced by eight electrons. The mean lifetime $\tau$ calculated by Saunders (1990) is

$$\tau \approx 2 \times 10^{-12} \text{ s.} \tag{7.41}$$

The deformation of clusters involves the electronic and phononic response of the system characterized by the times $10^{-15}$ s ($\approx 1$ eV) and $10^{-13}$ s ($\approx 10$ meV). Both these times are shorter than $\tau$ implying that one can use the Born–Oppenheimer (adiabatic) approximation for the description of a Coulomb explosion. The path to fission is determined by electronic level crossings rather than the inertia of the atomic nuclei. The fission decay rate for $Na_{10}^{+2}$ clusters is given by equation (7.22) with a preformation factor $P$, a knocking rate $f$ and a barrier penetration $T$. However, in this particular case, it is easier to calculate the product $PT$ than to calculate the factors separately. In other words $P(n = 3)$ (see below) provides a situation where the two clusters $Na_7^+$ and $Na_3^+$ are beyond the fission barrier, i.e. a quantity that also contains $T$.

Within the framework of the model discussed in the previous section one expects to find $n = 3$ level crossings in the process. From the potential energy surface displayed in Fig. 1 of Saunders (1990), and dividing the interval between the ground states and scission ($\approx 20$ Å) into three equal parts, one can calculate the restoring force in the harmonic approximation

$$\tfrac{1}{2}C\xi^2 = 0.1 \text{ eV} \quad \left(\xi = \tfrac{1}{3}\right), \tag{7.42}$$

leading to

$$C \approx 2 \text{ eV}. \tag{7.43}$$

The inertia of the motion is given by

$$\frac{D}{\hbar^2} = \frac{n^2}{2|v|} = \frac{4.5}{|v|}, \tag{7.44}$$

where $v$ is the matrix element responsible for the jump of two electrons from an occupied to an empty orbital, measured in eV.

Using $\omega = \sqrt{C/D}$ the knocking rate is determined by

$$f = \frac{\omega}{2\pi} \approx 0.16\sqrt{|v|}10^{15} \text{ s}^{-1}. \tag{7.45}$$

The formation probability of the outgoing cluster on the surface of the parent cluster is determined by the parameter $\alpha^2$ (see equation (7.21)) which in the present case is given by

$$\alpha^2 = \sqrt{\frac{C}{2|v|}}\, n = \frac{3}{\sqrt{|v|}}, \tag{7.46}$$

so that

$$P \approx \frac{1}{|v|^{1/4}} \exp\left(-\frac{3}{\sqrt{|v|}}\right). \tag{7.47}$$

The lifetime is then given by (see the discussion after equation (7.41) above)

$$\tau = (fP)^{-1} = \frac{\exp\left(\frac{3}{\sqrt{|v|}}\right)}{|v|^{1/4}} \times 6 \times 10^{-15} \text{ s}. \tag{7.48}$$

Setting this quantity equal to (7.41) one obtains $|v| \approx 0.3$ eV. Matrix elements of the order of 0.3 eV are typical for interaction among electrons. It is still an open question to what extent such matrix elements are related to pairing in clusters (Snider and Sorbello (1984), Mottelson (1992), Barranco *et al.* (1992), a subject which is closely related to that discussed in connection with equation (2.3) (see Satula *et al.* (1998)).